

## An Application of Self-similarity Analysis for Segmentation of Images of Human Liver

**K. Bartnykas, A. Ušinskas**

*Department of Electronic Systems, Vilnius Gediminas Technical University  
 Naugarduko 41 str., LT-03227 Vilnius, phone: +370 (5) 2744766, e-mail: kestutis.bartnykas@el.vgtu.lt*

### Introduction

Medical images are often treated as images having low contrast properties. While this is very important fact, it follows that images can be characterized by self-similarity feature also. Self-similarity refers to images that have several parts looking as the whole image. In mathematics self-similar geometrical objects are known as fractals. This feature can characterize all images which exist in nature, medical ones also [1]. Thus, it can be applied fractal-based approach for image analysis of such type. This is reason which makes fractal-based approach such attractive for analysis of medical images. This approach can be requested also because of the low contrast characteristic of the grayscale medical images. Object of interest are grayscale medical images of human liver. Then, this document is based on references [1-3] and it attempts to investigate exploitation possibility of self-similarity feature in medical images for discrimination of different tissues in image. This can be referred to segmentation task also. The main task behind this article is investigation of relevance of multifractal mathematical model for discrimination of different tissues of human liver.

Fractal is ideal case existing in mathematics. Unfortunately, the objects existing in nature have similar inner structure at different scales only in particular range of zooming scales. While fractals in real images are rare case, a multifractal term is introduced and applied in case of real images. This article refers to the image as texture consisting and texture analysis itself is fractal-based. A correlation between texture coarseness and fractal dimension of a texture is base for this approach.

There are a few articles that show an interest on applications of fractal theory on medical images. [1] explains mathematical concept of multifractal theory for segmentation task and exploits it on magnetic resonance imaging images of human brain. [3] proposes the method of self-similarity analysis applied to 2D breast cancer imaging.

Several works have dealt with human liver region segmentation problem. There are studies based on histogram analysis [4], active contours [5]. These works encounter the same problem, while these works exploits gray

level intensity alone. This is because of nearby organs having similar gray level intensity by which liver are surrounded. This makes difficult to segment liver region directly. Indeed the problem is solved by applying few pre-processing methods consecutively.

### Multifractal analysis basics

Suppose the image under investigation has size  $M \times N$ , then an image function can be described this way

$$I = \{(m, n, f(m, n)) \mid m \in [1, M], n \in [1, N]\}, \quad (1)$$

where  $f(m, n)$  – specifies the intensity of pixel  $(m, n)$ ,  $f(m, n) = \{z \in N_0 \mid z \leq 255\}$ .  $S$  is an integer space of pixel coordinates

$$S = \{(m, n) \mid m \in [1, M], n \in [1, N]\}, \quad (2)$$

The coast length example is frequently used to explain the fractal concept [6]. Suppose the measurement of coast length is taken repeatedly by applying a ruler of different length each time. It is apparent that decrease of ruler length produces increased length of coast under measurement. A relation between the measured coast length and the ruler length can be understand as estimate of the coast-line's geometrical properties such as roughness for example. This functional relationship can be expressed approximately in mathematical form by  $B_d(A) \propto N(\varepsilon)\varepsilon^d$  or after few minor changes by

$$N(\varepsilon) = \frac{c}{\varepsilon^d}, \quad (3)$$

where  $N(\varepsilon)$  – is the minimum number of plane elements of size  $\varepsilon$  required to cover the set  $A \subset R^n$ ,  $\varepsilon$  – the ruler length,  $c$  – mathematical constant. After few mathematical procedures, Eq. 3 can be replaced with an equivalent formula

$$d = - \lim_{\varepsilon \rightarrow 0} \frac{\ln(N(\varepsilon))}{\ln(\varepsilon)}. \quad (4)$$

This formula is main tool used in this research and is used in different mathematical form following the framework described below. This formula is referred to Hausdorff dimension also. More information for this in detail can be found in [7]. Usually, the framework for image analysis in multifractal theory terms is proposed as follows. Firstly, the coarse Hölder exponent is calculated which describes the point-wise singularity of the object. Secondly, the multifractal spectrum is calculated, which is derived as distribution of Hölder exponent, denoted as  $\alpha$ . While these quantities are estimated in discrete space because of discrete nature of digital image, the limit in Eq. 4 is not possible to estimate directly. Indeed the coarse Hölder exponent is estimated as follows

$$\alpha_i(m, n) = \frac{\ln(\mu_i(m, n))}{\ln(i)}, i = 1, 2, 3, \dots, \quad (5)$$

where  $\mu_i(m, n)$  is the quantity of measure in  $i \times i = \{(g, g) \mid g = 2p+1, p = 0, 1, 2, \dots\}$  sized neighbourhoods centered around each pixel of image. The limit of  $\alpha_i(m, n)$  is estimated then from bi-logarithmic graph  $\ln(\mu_i(m, n))$  vs.  $\ln(i)$  in sense of linear regression. After this procedure applied to whole image, the so called  $\alpha$ -image is obtained.

To calculate the distribution of  $\alpha$ -image, pooled  $\alpha$  values are discretized as follows

$$\alpha_r = \alpha_{\min} + (r-1)\Delta\alpha_r, r = 1, 2, 3, \dots, R, \quad (6)$$

where,  $R$  is the number of subranges in  $[\alpha_{\min}, \alpha_{\max}]$ . Division  $\Delta\alpha_r$  were used uniform as follows

$$\Delta\alpha_r = \alpha_r = (\alpha_{\max} - \alpha_{\min}) / R. \quad (7)$$

Then the  $\alpha$ -image is thresholded continuously in each subrange  $r$  leaving only those ‘‘active pixels’’ which lie in subrange  $[\alpha_r, \alpha_r + \Delta\alpha]$ . Then the dimension  $f(\alpha_r)$  of thresholded  $\alpha$ -image is calculated for each subrange according to formula

$$f_j(\alpha_r) = -\frac{\ln(N_j(\alpha_r))}{\ln(j)}, j = 1, 2, 3, \dots, \quad (8)$$

where  $N_j(\alpha_r)$  is number of boxes containing at least one  $\alpha$ -value belonging to the subrange  $[\alpha_r, \alpha_r + \Delta\alpha]$  when  $\alpha$ -image is covered with regular grid of boxes having size  $j$ .  $N_j(\alpha_r)$  is calculated repeatedly for different size of boxes  $j = \{1, 2, 3, \dots\}$  and  $f_j(\alpha_r)$  is then estimated from bi-logarithmic graph  $\ln(N_j(\alpha_r))$  vs.  $-\ln(j)$  in sense of linear regression. After examination of whole  $\alpha$ -image, the  $f(\alpha)$ -image is obtained by replacing the ‘‘active pixels’’ in each subrange  $[\alpha_r, \alpha_r + \Delta\alpha]$  with related value of  $f(\alpha)$ .

As depicted in [1], Eq. 5 merely describes relation of two quantities: the number of non-empty boxes and their dimension. It follows that each subset of pixels is defined only by two states i.e. black and white. Such an approach for calculation of fractal dimension can't lead to a reasonable result. Reasonable effect can be achieved using more general quantities, which are known as measures in mathematics. This article exploits four mostly used measures:

$$\text{Maximum} : \mu_i(m, n) = \max_{(k,l) \in \Omega} g(k, l), \quad (9)$$

$$\text{Minimum} : \mu_i(m, n) = \min_{(k,l) \in \Omega} g(k, l), \quad (10)$$

$$\text{Sum} : \mu_i(m, n) = \sum_{(k,l) \in \Omega} g(k, l), \quad (11)$$

$$\text{Iso} : \mu_i(m, n) = \text{Card}\{(k, l) \mid g(m, n) \equiv g(k, l), (k, l) \in \Omega\} \quad (12)$$

where  $\mu_i(m, n)$  – indicates capacity measures.  $g(k, l)$  – indicates gray-scale intensity values of pixels  $(k, l)$  belonging to the set of neighborhoods  $\Omega$  having size  $i$ .  $g(k, l)$  does not take zero value in case of measure. All of them give different information on the singularities encountered.

## Methodology

The aim is to prove if different kind of tissues can be distinguished using multifractal spectra. The spectrum is obtained for three different types of tissue: normal liver tissue (sample 1), tumor tissue (sample 2), and adjacent to the liver tissue (sample 3) (Fig. 1 and 3, first row). Samples of size  $64 \times 64$  representing these tissues are taken from CT images. Fig. 2 presents the results for samples taken from the first original CT image and Fig. 4 depicts results taken from the second original CT image. We need to adjust some of the parameters to apply implemented method on real images. The sum-measure is used and the square shape like for sliding window is used. We choose to replicate the image across its outer borders to deal padding problem with. Neighbourhood sizes for images of size  $64 \times 64$  are  $i = \{1, 3, 7, 15, 31\}$  while  $R$  value used to discretize  $\alpha$  into subranges is equal to 12. The number of subintervals  $R$  should also be properly chosen because it has an impact to the accuracy of the multifractal spectrum. Bigger number of subintervals gives erratic spectrum and smaller number of subintervals gives smoother spectrum. While spectra should preserve its smooth shape, it should have high enough resolution also. Sizes of boxes for box-dimension are  $j = \{2, 4, 8, 16, 32, 64\}$  that is natural series with elements increasing by power of two.

## Results

According to [1], the graph of  $f(\alpha)$  is continuous function of  $\alpha$  and has the parabolic shape which is typical for a number of subjects existing in nature. Medical images reside in this group also. Usually, the peak of the graph is near  $\alpha = 2$  for two-dimensional signals. The  $\alpha$ -value holds local information of the image. Each pixel of the image is defined by its own coarse Hölder exponent  $\alpha$ . Subsets of image space  $S$  having similar  $\alpha$ -value, have the same scaling behaviour and share similar qualities. These, in context of segmentation, define meaningful objects which reside in the image. The objects in fractal-based image segmentation task are boundaries of an object. The subsets consisting of the pixels having  $\alpha \approx 2$  make homogeneous regions, the measure is regular. The subsets consisting of the pixels having  $\alpha \ll 2$  or  $\alpha \gg 2$  indicates that pixel has irregular measure. This means, that such pixel is included in subset with high gradient or subset which can be interpreted as discontinuous signal. Here can be found singularities such as lines, step-edges, and corners.

However, only local interpretation of  $\alpha$ -value is not always sufficient to get reasonable results. Indeed, it is used interpretation of  $f(\alpha)$ -value along with mentioned one i.e.  $\alpha$ -value. Value  $f(\alpha)$  holds global information of the image.

Using statements described above, let us compare the spectra in Fig. 2. Comparison of these spectra gives following findings. The peaks of the spectra are at three different  $\alpha$ -values. Sample 1 has the peak at  $\alpha = 1.9993$ , sample 2 has the peak at  $\alpha = 1.9922$ , and sample 3 has the peak at  $\alpha = 2.0123$ . This shows us that samples under investigation belong to three different types of tissue. The peak value of  $f(\alpha)$  is approximately 0.7 that according to the statements above gives no meaningful information about the samples. Similar pattern can be seen behind Fig. 4 also. Samples from 1 to 3 have the peaks at  $\alpha = 1.9928$ ,  $\alpha = 1.9873$ ,  $\alpha = 1.9685$  values respectively. Recall, that samples depicted in his figure are taken from another slice belonging to the same pool of CT images. To have stronger

evidence, statistics is shown in Table 1. It is seen that these data are consistent with the numbers taken from Fig. 2 and Fig. 4.

**Table 1.** Statistics made on three different  $\alpha$ -values of interest. 30 different samples are used to calculate the mean.

Statistical description	Sample 1 (liver)	Sample 2 (tumour)	Sample 3 (abdomen)
Mean	1.9994	1.9974	1.9918
Std.	0.0054153	0.0069620	0.019258

Result produced by multifractal segmentation method applied on medical liver image (Fig. 5(a)) is presented in Fig. 5(b). Segmented image was produced by estimating minimum measure (Eq. 9) of negative image, then thresholding this image. Anisotropic diffusion was taken as a preprocessing step to contract the light intensity dispersion of the parenchyma which results in enhanced contrast of the image.

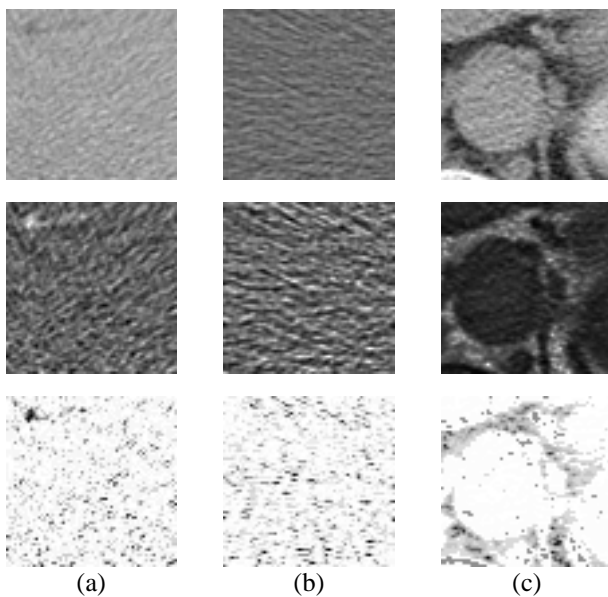


**Fig. 1.** Three types of the tissue under investigation for three samples, first row: a) liver – sample 1, b) tumour – sample 2, c) surrounding tissues i.e. abdomen – sample 3.  $\alpha$ -images, second row.  $f(\alpha)$ -images, third row

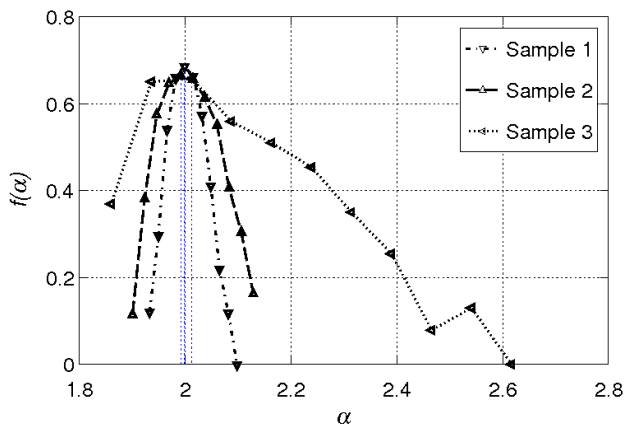


**Fig. 2.** Multifractal spectra of the tissues under investigation for three samples taken from some slice of pool of CT images

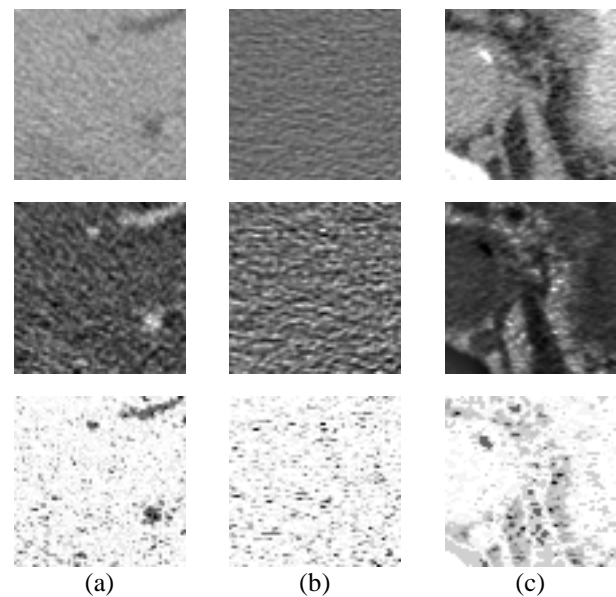


**Fig. 3.** Three types of the tissue under investigation for three samples, first row: a) liver – sample 1, b) tumour – sample 2, c) surrounding tissues i.e. abdomen – sample 3.  $\alpha$ -images, second row.  $f(\alpha)$ -images, third row. Samples are taken from another slice of pool of CT images

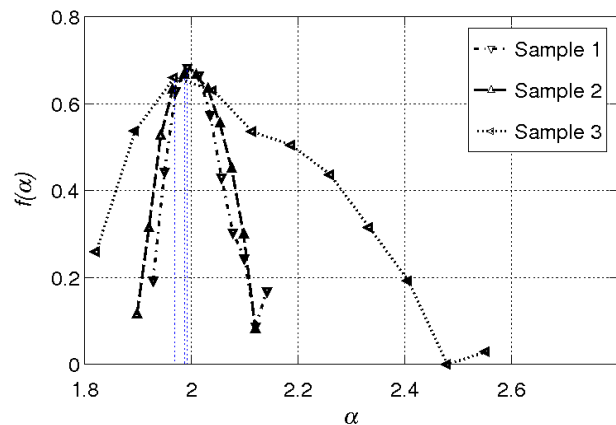


**Fig. 4.** Multifractal spectra of the tissues under investigation for three samples taken from another slice of CT images

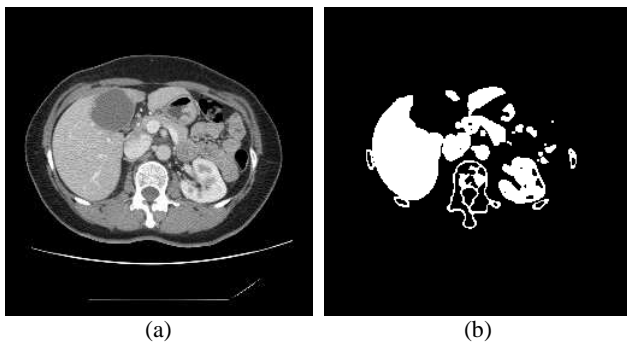


Fig. 5. Original image with thresholded image: a) original image, b) segmentation result

## Conclusions

The most appropriate set of settings to the problem under interest are: sum-measure, replicate padding, neighbourhood sizes suitable for images of size  $64 \times 64$  are  $i = \{1, 3, 7, 15, 31\}$ , number of subranges for images of size  $64 \times 64$  is equal to  $R = 12$ , sizes of boxes for box-dimension suitable for images of size  $64 \times 64$   $j = \{2, 4, 8, 16, 32, 64\}$ .

Spectra  $f(\alpha)$  of all three investigated tissue have the maximum at different  $\alpha$ -values (Fig. 2 and 4) what suggests that multifractal theory can be valuable tool to describe human's liver tissues in CT images. However, these  $\alpha$ -values are very close each other that can be due to estimation inaccuracy of  $\alpha$ -value or because of inefficient res-

olution of spectra. Presentation of segmentation results is also given (Fig. 5(b)).

## References

1. **Reljin I., Reljin B.** Fractal geometry and multifractals in analyzing and processing medical data and images // *Archive of Oncology*. – 2002. Vol. 10. – P. 283-293
2. **Nilsson E.** Multifractal-based Image Analysis with applications in Medical Imaging // *Master's Thesis in Computing Science and Mathematics*. – 2007.
3. **Stojić T., Reljin I., Reljin B.** Adaptation of multifractal analysis to segmentation of microcalcifications in digital mammograms // *Physica A: Statistical Mechanics and its Applications*. – 2006. Vol. 367. – P. 494-508
4. **Bae KT, Giger ML, Chen CT, Kahn CE** Automatic Segmentation of liver structure in CT images. // *Med Phys*. – 1993. – Vol. 20. – P. 71-78
5. **Lapeer R. J, Tan AC, Aldridge R.** A combined approach to 3D medical image segmentation using marker-based watersheds and active contours: the active watershed method. // *Springer*. – 2006. Vol. 2488. – P. 596-603
6. **Sonka M., Hlavac V., Boyle R.** *Image Processing, Analysis, and Machine Vision* // *Thomson Learning*, 2008.
7. **Кроновер Р. М.** Фракталы и хаос в динамических системах // *Москва: Технофера*, 2006.

Received 2008 10 10

**K. Bartnykas, A. Ušinskas. An Application of Self-similarity Analysis to Segmentation of Images of Human Liver // *Electronics and Electrical Engineering*. – Kaunas: Technologija, 2009. – No. 2(90). – P. 35–38.**

Images of human liver taken from computed tomography are considered. These images are analysed as self-similar sets. To accomplish this analysis, the multifractal mathematical model is applied. The main task behind this article is investigation of relevance of multifractal mathematical model for discrimination of different tissues of human liver. Indeed, we need to show that a multifractal spectrum allows us to distinct different types of tissues. This allows us to suggest application of multifractal model for image segmentation task. Using multifractal spectra was shown that three different types of tissues can be identified. Types of tissues under investigation were: liver, tumour, and surrounding tissues i.e. abdomen. Ill. 5, bibl. 7 (in English; summaries in English, Russian and Lithuanian).

**К. Бартникас, А. Ушинскас. Применение анализа самоподобных множеств для сегментации изображений печени человека // *Электроника и электротехника*. – Каунас: Технология, 2009. – № 2(90). – С. 35–38.**

Анализируются изображения компьютерной томографии, отображающие печень человека. Эти изображения анализируются как самоподобные множества, применяя математическую модель мультифракталов. Исследование концентрируется на проверку годности математической модели фракталов для отделения друг от друга различных тканей печени и соседних для них тканей. Для того показано, что фрактальная гистограмма позволяет разделить друг от друга эти ткани. Это также позволяет думать о возможности применить данную модель для сегментации исследуемых тканей. Проанализовав три различные ткани, выяснилось, что это может быть сделано воспользуясь фрактальной гистограммой. Исследуемые ткани есть: печень, навик и соседняя для печени ткань. Ил. 5, библи. 7 (на английском языке; рефераты на английском, русском и литовском яз.).

**K. Bartnykas, A. Ušinskas. Į save panašių aibių taikymas žmogaus kepenų atvaizdams segmentuoti // *Elektronika ir elektrotechnika*. – Kaunas: Technologija, 2009. – Nr. 2(90). – P. 35–38.**

Žmogaus kepenų kompiuterinės tomogramos atvaizdai analizuojami kaip į save panašios aibės. Šiai analizei atlikti taikomas multifraktalų matematinis modelis. Tyrimu siekiama išsiaiškinti, ar, taikant fraktalų matematinį modelį, įmanoma atskirti skirtingus kepenų audinius. Tam taikoma fraktalinė histograma ir, jeigu ji padeda atskirti nagrinėjamų tipų audinius, tai leidžia manyti, kad, naudojant taikomą metodą, taip pat galima šių tipų audinius segmentuoti. Naudojant fraktalinę histogramą, galima atskirti trijų nagrinėtų tipų audinius: kepenų navikus, kepenims gretimus audinius. Il. 5, bibl. 7 (anglų kalba; santraukos anglų, rusų ir lietuvių k.).